Dynamics of math xmlns="http://www.w3.org/1998/Math/MathML">mmultiscripts>mi>He/mi>mprescripts>/mprescripts>none>/none>mn>3/mn>/mmultiscripts>/math> in one dimension in the Luttinger liquid limit

J. Adams, M. Lewkowitz, C. Huan, N. Masuhara, D. Candela, and N. S. Sullivan

Phys. Rev. B **106**, 195402 — Published 3 November 2022

DOI: 10.1103/PhysRevB.106.195402

Dynamics of ^{3}He in One Dimension in the Luttinger-Liquid Limit.

J. Adams,[1] M. Lewkowitz,[1] C. Huan,[1] N. Masuhara,[1] D. Candela,[2] and N. S. Sullivan[1,*]

[1]*Department of Physics and National High Magnetic Field Laboratory, University of Florida, Florida 32611, USA*
[2]*Department of Physics, University of Massachusetts, Amherst, Massachusetts 01003, USA*

(Dated: October 24, 2022)

NMR techniques have been used to investigate the dynamics of highly degenerate ^{3}He confined to the interior of ^{4}He plated nanotubes of MCM-41. The ^{3}He line density was 0.93 ± 0.10 nm^{-1}, corresponding to a Fermi degeneracy temperature of $T_F \approx 0.1$ K. Experiments conducted down to 10 mK reveal a linear temperature dependence of the nuclear spin-lattice relaxation for $T < T_F$, following a peak at $2T_F$, which are hallmarks of Luttinger liquid physics .

PACS numbers: 67.80.bd, 67.30.hm, 76.60.-k
Keywords: Luttinger liquid, NMR, Fermi temperature, nanochannel

INTRODUCTION

New physical properties are predicted for systems constrained to one dimension (1D) for which correlations between neighbors render all excitations collective, and so must be described by Tomonaga-Luttinger liquid (TLL) theory [1–3]. While considerable activity has been dedicated to electronic systems (quantum Hall edge states [4] and quantum wires [5]) much less attention has been given to neutral systems [6, 7]. Among neutral systems, 1D quantum gases are of particular interest because of their high purity, well-characterized interactions and the ability to vary the density continuously. One dimensional ^{4}He superfluidity has been observed in nanotubes [8–12] and the onset of quantum degeneracy has been reported for ^{3}He in the nanoscale channels of FSM16 [13, 14].

Previous studies of ^{3}He on MCM-41 focused on temperatures $T > T_F$ [15–17] successfully demonstrated the classical behavior expected for quasi-1D spin-1/2 systems such as the $t^{\frac{1}{2}}$ power law for the temporal dependence of the spin diffusion in the 1D hydrodynamic limit [15], but have not explored the system when highly degenerate. Here we report a significant improvement over earlier NMR studies of ^{3}He on MCM-41 [18, 19] by mixing fine Ag powder to better thermalize the system at low temperatures, enabling studies of the dynamics well below the Fermi temperature. Matsushita *et al.* [20] have recently reported 1D behavior for NMR studies of ^{3}He adsorbed on a different material, FSM-16, for a wide range of line densities for temperatures $T \geq 60$ mK, both above and below T_F. However, their results for an NMR frequency of 4.4 MHz show a different temperature dependence for the relaxation times compared to our observations at 45 MHz, suggesting a variation of the spectral density of the dynamics as a function of frequency.

One unique characteristic of 1D Fermi spin systems, used as a hallmark for detecting TLL behavior, is a linear dependence of the relaxation times on temperature [21], at low temperatures with a peak in the relaxation time at $T = 2T_F$, provided the spin polarization is not high [22]. Although a linear temperature dependence of ^{3}He relaxation has been observed for liquid ^{3}He in contact with a solid surface [23] it is uniformly linear for $0.7 < T < 700$ mK with no peak and that dependence results from the static Pauli susceptibility of the bulk liquid ^{3}He which is not present in the experiments described here.

The unusual dynamical behavior at low temperatures for Luttinger liquids results naturally from the density of states in low density 1D Fermi systems which varies as $\rho(E) \propto E^{-\alpha}$ [24] where the power α is related to the Luttinger liquid parameter K [24] by $\alpha = \frac{1}{2}(K + K^{-1} - 2)$. K is the ratio of the Fermi velocity to the speed of sound [6]. For ^{3}He line densities $n \approx 1.0$ nm^{-1}, as used in experiments reported here, Astrakharchik and Boronat [6] show $K \approx 1.3$ for which $\alpha = 0.03$.

Detailed calculations by Polini and Vignale [21] for charged systems show that there is a peak in the relaxation rate at $T = 2T_F$ followed at higher temperatures by a $T^{-\frac{1}{2}}$ dependence. The latter is expected from the chemical potential in the non-degenerate regime $\mu = \frac{k_b T}{2} \ln\left(\frac{16 T_F}{\pi T}\right)$. Earlier NMR studies [19, 25] were carried out close to T_F and while consistent with the predictions of Polini and Vignale [21] those studies did not explore temperatures significantly below the T_F due to inadequate thermalization. For the present experiments a new experimental cell with greatly improved thermalization was constructed.

EXPERIMENTAL METHODS

The quasi-1D confinement of ^{3}He atoms in this experiment was provided by mesoporous silicate MCM-41 [26], which consists of hexagonal channels of diameter 2.3-2.7 nm (with largest inscribed circles of 2.1-2.4 nm) and $\approx$ 300 nm in length. To enable cooling the system to much lower temperatures than in earlier experiments, the MCM-41 grains were mixed with ultra-fine (sub-μm Ag) powder [27] and this mixture was pressed into the polycarbonate NMR cell with a pressure of about 20 bar to make thermal contact with a solid silver post extending from a copper nuclear refrigerator. The nuclear refrigerator was cooled to temperatures down to 3 mK, but Kapitza thermal resistance between the Ag powder and the MCM-41 prevented reliable cooling of the ^{3}He below 5-10

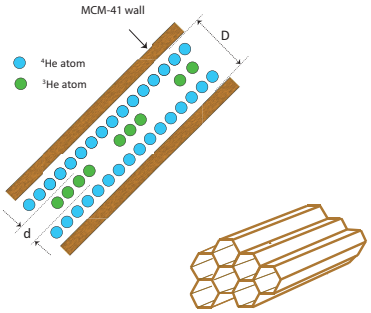

FIG. 1. (Color online) Illustration showing a cross-section of one hexagonal nanotube of MCM-41 with ^{4}He plating (blue) and internal ^{3}He atoms (green). D, the largest inscribed circle, is 2.1-2.4 nm, and following the arguments of Matsushita *et al.* [8, 9], the diameter accessible to ^{3}He atoms is 0.8-1.1 nm. The inset at the lower right side illustrates the typical stacking of the nanochannels as large bundles of nanotubes with a given orientation.

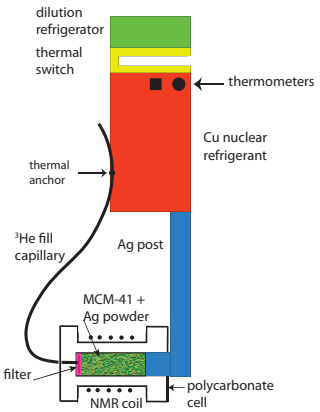

FIG. 2. (Color online) Schematic representation (not to scale) of the low temperature NMR cell and link to a solid silver cold finger extending from a nuclear refrigerator [41, 42]. The copper nuclear refrigerator was used in this experiment for temperatures below 11 mK. The high purity annealed Cu and high purity silver post provided an excellent thermal link between the thermometers and the NMR cell.

mK (see supplemental material [28], and also the references [8, 9, 27, 29–35] therein). The temperatures were recorded using a RuO_2 thermometer [36] for $0.03 < T < 1.0$ K and also a ^{3}He melting curve thermometer [37] for $T < 0.25$ K. After mounting the cell on the experimental cold finger (Fig. 2) the entire unit was heated to 373 K and pumped for 8 hours to remove adsorbed water and air, before cooling to cryogenic temperatures. For a review of adsorption on MCM-41 see Nichols *et al.* [38]

A key feature of this experiment was pre-plating of the MCM-41 substrate with a carefully determined quantity of ^{4}He, which produces no NMR signal, before admitting the ^{3}He sample (Fig. 1). The ^{4}He plating serves two purposes, both of which enable the system to better approximate an ideal 1D gas of ^{3}He atoms: (a) by reducing the effective diameter d of the channels, the gap Δ_{01} to the first excited transverse quantum states is increased to far above the lowest temperatures used, and (b) the ^{3}He-(MCM-41) wall interaction is replaced by the much weaker ^{3}He-^{4}He interaction [9, 33, 39].

The NMR cell contained 0.070 g of MCM-41 and 0.42 g of Ag powder. From the adsorption isotherm the monolayer completion corresponds to a total MCM-41 surface area of 61.1 $\pm$ 2.4 m^2. From the manufacturer's specification [27] the surface area of the Ag powder was 0.88 m^2, or about 1.4% of the total area. (The surface area of the cell wall and the filter are estimated to be less than 0.1 m^2.) Following Matsuhara *et al.* [13, 40] the line density is given by $n_L = \frac{N_3}{S}\pi D$ where N_3 is the number of ^{3}He atoms, S is the available surface area, and D is the diameter of the nanotubes prior to plating. From the value of D = 2.5 $\pm$ 0.3 nm we find $n_L = 0.93 \pm 0.10$ nm^{-1}.

A ^{3}He isotherm measurement was carried out at 1.5 K to determine a monolayer coverage and the coverage for the minimum compressibility. (See supplemental material [28].) From the ratio of the monolayer coverage and the minimum compressibility determined from the isotherm one can use the method of Matsushita *et al.* [8, 9] to estimate the free diameter for the ^{3}He inside the pore. Note that the repulsive range of the He-He interactions is of the order of 0.30 - 0.35 nm which is significantly larger than the size of the atoms. With this in mind we find a pore diameter $d \approx 0.80$ - 1.1 nm which determines the first excited energy level Δ_{01} for the transverse motion of the atoms. For this value of d $\Delta_{01}/k_B \approx 0.7$ K, comparable to the values given by Wada and Cole [9]. The system can be considered quasi-1D at temperatures well below Δ_{01} as there is very little excitation to transverse modes. For a line density of 0.93 nm^{-1} the Fermi temperature $T_F \approx 120$ mK (for an effective mass $m^*/m = 1.4$) and we have the desired condition $k_B T_F << \Delta_{01}$ for the observation of TLL dynamics.

For the NMR studies we employed a single coil resonated at 44.9 MHz and matched to a 50 ohm RF cable by a capacitive transformer [18] (not shown in Fig. 2). There was a significant loss in signal to noise compared to previous experiments due to the effect of the Ag powder, and the NMR line was appreciably broadened. An on-resonance $\pi/2$ RF pulse would lead to excessive RF heating and we therefore used an off-resonance technique with a small RF level to provide a large effective field in the rotating frame to produce modulated NMR echos using a two pulse sequence. (See supplemental material [28] for NMR details).

EXPERIMENTAL RESULTS

The nuclear spin-lattice relaxation time was determined by measuring the NMR echo amplitudes $M(t_W)$ for a series of RF pulse sequences: $(\frac{\pi}{2} - \tau - \pi)$ separated by t_W. The results shown in Fig. 3 are for the decay $1 - M(t_W)/M_0$ where M_0 is the equilibrium value for very long waiting times t_W.

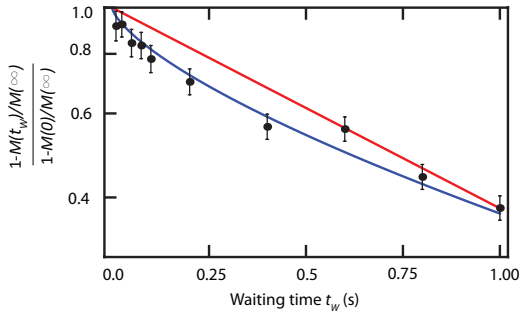

FIG. 3. (Color online) Comparison of the observed relaxation of the nuclear magnetization $M(t_W)$ (solid black circles) with a stretched exponential decay: $\exp[-(\frac{t_W}{T_1})^\beta]$ for β = 0.7 (solid blue line, best fit) and with pure exponential decay (solid red line) for β = 1.0 for a sample at 25 mK. For this sample the pure exponential decay does not provide a good fit to the data. Additional examples for other temperatures are given in the supplementary material. Note that while ideally $M(0) = 0$, small non-zero values occur due to the limitations on RF pulse amplitude to prevent unacceptable heating. (t_W is the waiting time between pulse sequences.)

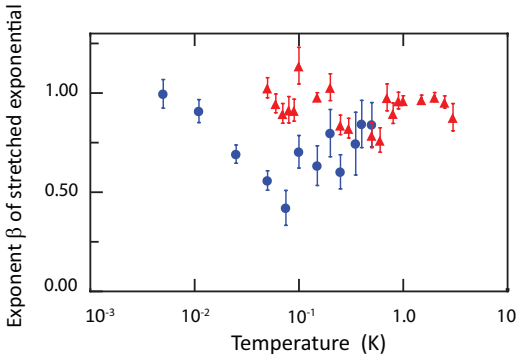

FIG. 4. (Color online) Variation of the exponent (β) for the stretched exponential fit to the magnetization relaxation as a function of temperature. The solid black circles are for the sample with Ag powder and the solid red triangles are for an earlier sample [18] without Ag powder.

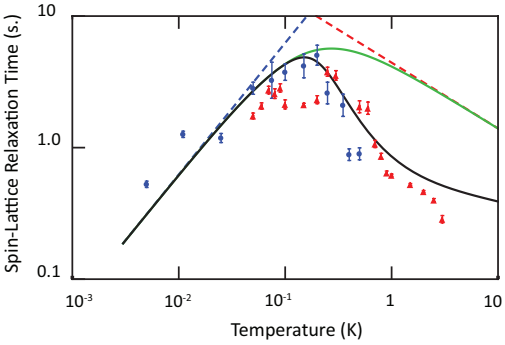

FIG. 5. (Color online) Observed temperature dependence of the nuclear spin-lattice relaxation times for the new sample with Ag powder (solid blue circles) compared to the earlier sample without Ag powder (solid red triangles). The broken blue line depicts the limiting behavior $T_1 \propto T$ at low temperatures and the broken red line is $T_1 \propto T^{-1/2}$ for high temperatures. The best overall fit to the data is for $T_F = 95 \pm 5$ mK. The solid green line is the theoretical dependence from Polini and Vignale [21] that does not include transverse excitations, and the solid black line is the dependence if excitations to the lowest transverse mode mode with $\Delta_{01}/k_B = 0.77$ K are included. Typical error bars are shown for the two sets of data.

At low temperatures $T < T_F$ the relaxation was not purely exponential and a better fit is obtained for a stretched exponential $\exp[-(\frac{t_W}{T_1})^\beta]$. In addition to Fig. 3 we have included in the supplemental material similar analyses of the NMR decay in terms of pure and stretched exponentials for $T = 5$ mK, 11 mK and 200 mK. This non-exponential relaxation is not unexpected and was previously observed by Matsushita *et al.* [20] for the T_2 relaxation of ^{3}He on ^{4}He-plated FSM-16. The nuclear spin-spin relaxation T_2 is determined by fluctuations at zero and very low frequencies and can be influenced by static wall impurities. In our case we observed stretched exponential relaxation for measurements of T_1 which is associated with the density of fluctuations of the ^{3}He atoms at high frequencies such as those due to ^{3}He - ^{3}He collisions. In that case the relaxation is expected to be dominated by pure ^{3}He-^{3}He dipolar interactions which vary as $(3\cos^2\theta_i - 1)$ where θ_i is the angle of the orientation of a particular nanotube with respect to the applied magnetic field. Because of the variation of θ_i throughout the sample there is a distribution of relaxations times and an overall stretched exponential response is expected.

Stretched exponential decay has also been seen for nanoconfined water [43] and is universally observed in hierarchically constrained systems[44] such as molecular and electronic glasses [45], mathematical simulations of frustrated systems [46] and for defect diffusion in many systems [47]. If the relaxation dynamics in Luttinger liquids is hierarchical, for which low energy barriers must be crossed before high energy barriers [48, 49], a stretched exponential decay can be expected. The variation of the stretched exponential coefficient, β, as a function of temperature is shown in Fig. 4.

Above the region of degeneracy ($T > T_F$) a straight exponential provides the best fit to the data while β approaches 0.4 at temperatures ≈ 0.05 K but returns to values near unity at the lowest temperatures. Fig. 5 shows the data for this experiment analyzed allowing non-exponential decay. Also shown (as red triangles) is the previous data [18] but now analyzed for consistency allowing non-exponential decay.

DISCUSSION

The detailed calculations of Polini and Vignale [21] lead to an intrinsic spin (or "spin drag") relaxation rate

$$\tau_S^{-1} = \frac{8}{9\pi}\gamma_{2k_F}^2 \frac{T}{2T_F}\frac{E_F}{\hbar} \qquad (1)$$

where $\gamma_{2k_F} = mg_{1D}/n_L\hbar^2$ is the dimensionless Yang interaction parameter (evaluated at momentum transfer $q = 2k_F$) and g_{1D} is the s-wave interaction strength. $E_F = k_BT_F$ is the Fermi energy. The resulting nuclear spin-lattice relaxation time $T_1 = \tau_S^{-1}/M_2$ where $M_2 = 1.8 \times 10^8\,\mathrm{s}^{-2}$ is the NMR second moment (see supplemental material information [28]), or

$$T_1 = \frac{8}{9\pi}\gamma_{2k_F}^2 \frac{T}{2T_F}\frac{E_F}{\hbar M_2} \tag{2}$$

The best fit to the experimental data at low temperatures (shown by the solid black line in Fig. 5) is for $T_1 = 25\frac{T}{2T_F}$ or $\gamma_{2k_F} = 0.54 \pm 0.07$. This value of γ is smaller than that obtained for the experiments on adsorbed ^{3}He without Ag powder [19], and the difference is attributed to a better evaluation of the effect of the transverse excitations in the new sample for $T > T_F$. It should be noted that if the characteristic correlation time $\tau > \omega_L^{-1}$ (the inverse of the Larmor frequency) the temperature dependence of T_1 is typically different to that of the spin-spin relaxation time, T_2. Basically, T_1 measures the spectral density of the fluctuations at high frequencies while T_2 measure the density at low frequencies and will be influenced by low rate processes such as diffusion of ^{3}He impurities in the ^{4}He wall layer and not reflect the Luttinger dynamics.

At high temperatures the presence of thermal excitations of transverse modes in the nanochannels provides an additional relaxation path and therefore reduces the relaxation time below that calculated by Polini and Vignale [21] who found

$$\tau_{HT}^{-1} = \frac{16}{\pi^{7/2}}\gamma_0^2\left[\frac{T}{2T_F}\right]^{-1/2}\frac{E_F}{\hbar} \tag{3}$$

using a high temperature chemical potential $\mu_S = \frac{k_BT}{2}\ln\left[\frac{2\pi\hbar^2}{mk_BT}\right]$ which yields the broken red line in Fig. 5 given by $T_1 = 7.0[\frac{T}{2T_F}]^{-1/2}$. The addition of the transverse excitations adds the term Δ_{01} to the the thermal factor $\exp\left[-(E + \Delta_{01} - \mu)/k_BT\right]$. The calculated value of Δ_{01}/k_B was 0.68K following the assumptions about the free diameter inside the MCM-41 channels discussed in section II.

Adding all contributions, we find the solid black curve for $\Delta_{01} = 0.77$ K and $\gamma_0 = 0.47 \pm 0.07$. This fit is in reasonable agreement with the experimental data provided we use stretched exponentials to describe the relaxation data. As Δ_{01} is very sensitive to the effective channel diameter d, the difference between the best fitted value 0.77 K and the calculated value 0.68 K is not surprising.

CONCLUSION

Measurements of the nuclear spin-lattice relaxation times for ^{3}He confined to the interior of ^{4}He plated nanochannels of MCM-41 show a linear dependence on temperature when the sample is cooled well below the degeneracy temperature, T_F. Below T_F the relaxation follows a stretched exponential decay as expected for system constrained to hierarchical dynamics. At high temperatures the expected $T^{-1/2}$ dependence is strongly modified by the excitation of transverse motions starting at the lowest excitation energy Δ_{01}. The peak in the value of the relaxation time clearly identifies the degeneracy temperature and the value deduced is consistent with the line density of the sample. These behaviors are in good agreement with the theory of Polini *et al.* [21] for Luttinger liquid dynamics, and this appears to be one of the first measurements of such dynamics in a neutral fermion system well below T_F.

This research was carried out at the NHMFL High B/T Facility which is supported by NSF Grant DMR 1644779 and by the State of Florida. This project was supported in part by an award from the Collaborative Users Grant Program of the NHMFL. We gratefully acknowledge useful discussions with Brian Cowan, Dmitrii Maslov, Henri Godfrin, Pradeep Kumar and Giovanni Vignale.

* sullivan@phys.ufl.edu

[1] T. Giamarchi, *Quantum Physics in One Dimension* (Clarendon Press, Oxford, 2003).
[2] S.-i. Tomonaga, Remarks on Bloch's Method of Sound Waves applied to Many-Fermion Problems, Progress of Theoretical Physics **5**, 544 (1950), https://academic.oup.com/ptp/article-pdf/5/4/544/5430161/5-4-544.pdf.
[3] J. M. Luttinger, An exactly soluble model of a many-fermion system, J. Math. Phys. **4**, 1154 (1963).
[4] M. Hashisaka and T. Fujisawa, Tomonaga Luttinger liquid nature of edge excitations in integer quantum Hall edge channels, Rev. in Phys. **3**, 32 (2018).
[5] D. Laroche, G. Gervais, M. P. Lilly, and J. L. Reno, 1D-1D Coulomb drag signature of a Luttinger liquid, Science **343**, 631 (2014), https://www.science.org/doi/pdf/10.1126/science.1244152.
[6] G. E. Astrakharchik and J. Boronat, Luttinger-liquid behavior of one-dimensional ^{3}He, Phys. Rev. B **90**, 235439 (2014).
[7] E. Krotscheck and M. D. Miller, Properties of ^{4}He in one dimension, Phys. Rev. B **60**, 13038 (1999).
[8] N. Wada and M. W. Cole, Low-dimensional helium quantum fluids realized under nano-extreme conditions, J. Phys. Soc. Jpn. **77**, 111012 (2008)).
[9] N. Wada, T. Matsushita, M. Heidi, and R. Toda, Fluid states of helium adsorbed in nanopores, J. Low Temp. Phys. , 324 (2009).
[10] J. Taniguchi, R. Fujii, and M. Suzuki, Superfluidity and BEC of liquid ^{4}He confined in a nanometer-size channel, Phys. Rev. B **84**, 134511 (2011).
[11] N. Wada, M. Hieda, R. Todab, and T. Matsushita, Observation of superfluidity in two- and one-dimensions, Low Temp. Phys. **39**, 786 (2013).
[12] P. F. Duc, N. Savard, M. Petrescu, B. Rosenow, A. D. Maestro, and G. Gervais, Critical flow and dissipation in a quasi–one-dimensional superfluid, Science Advances **1**, 10.1126/sciadv.1400222 (2015).
[13] Y. Matsushita, J. Taniguchi, A. Yamaguchi, H. Ishimoto, H. Ikegami, T. Matsushita, N. Wada, S. M. Gatica, M. W. Cole, and F. Ancilotto, Dimensional-crossover of 3He gas formed in one-dimensional nanometer tunnel., J. Low Temp. Phys. **138**,

211–216 (2005).
[14] J. Taniguchi, A. Yamaguchi, H. Ishimoto, H. Ikegami, T. Matsushita, N. Wada, S. M. Gatica, M. W. Cole, F. Ancilotto, S. Inagaki, and Y. Fukushima, Possible one-dimensional ^{3}He quantum fluid formed in nanopores, Phys. Rev. Lett. **94**, 065301 (2005).
[15] B. Yager, J. Nyéki, A. Casey, B. P. Cowan, C. P. Lusher, and J. Saunders, NMR signature of one-dimensional behavior of ^{3}He in nanopores, Phys. Rev. Lett. **111**, 215303 (2013).
[16] A. P. Birchenko, N. P. Mikhin, A. S. Neoneta, E. Y. Rudavskii, and Y. Y. Fysun, Nuclear magnetization of ^{3}He adsorbed by the nanostructured material MCM-41, Low Temp. Phys. **44(5)**, 420 (2018).
[17] A. P. Birchenko, N. P. Mikhin, E. Y. Rudavskii, and Y. Y. Fysun, Spin diffusion in ^{3}He, Adsorbed nanostructured material MCM-41, Low Temp. Phys. **44(8)**, 755 (2018).
[18] C. Huan, J. Adams, M. Lewkowitz, N. Masuhara, D. Candela, and N. S. Sullivan, Nuclear spin relaxometry of ^{3}He atoms confined in mesoporous MCM-41, J. Low Temp. Phys. **196**, 308 (2019).
[19] C. Huan, J. Adams, M. Lewkowitz, N. Masuhara, D. Candela, and N. S. Sullivan, NMR studies of the dynamics of 1D ^{3}He in ^{4}He plated MCM-41, J. Low Temp. Phys. **201**, 146 (2020).
[20] T. Matsushita, R. Shibatsuji, K. Kurebayashi, K. Amaike, M. Hieda, and N. Wada, Temperature-linear spin-spin relaxation rates of one-dimensional ^{3}He fluid formed in nanochannels, Phys. Rev. B **103**, L241403 (2021).
[21] M. Polini and G. Vignale, Spin drag and spin-charge separation in cold Fermi gases, Phys. Rev. Lett. **98**, 266403 (2007).
[22] D. Rainis, M. Polini, M. P. Tosi, and G. Vignale, Spin-drag relaxation time in one-dimensional spin-polarized Fermi gases, Phys. Rev. B **77**, 035113 (2008).
[23] P. C. Hammel and R. C. Richardson, Relaxation of nuclear magnetization of liquid ^{3}He in confined geometries, Phys. Rev. Lett. **52**, 1441 (1984).
[24] S. Eggert, One-dimensional quantum wires: A pedestrian approach to bosonization (2009), arXiv:0708.0003 [cond-mat.str-el].
[25] C. Huan, N. Masuhara, J. Adams, M. Lewkowitz, and N. S. Sullivan, Probing the dynamics of 3He atoms adsorbed on MCM-41 with pulsed NMR, Journal of Physics: Conference Series **969**, 012001 (2018).
[26] *Type 643645*, Sigma Aldrich Corp., St. Louis, MO, USA.
[27] *Ames Advanced Materials*, South Glenns Falls, NJ 07080, grade K1-ED.
[28] See supplemental material at http://link.aps.org/??
[29] H. Ikegami, T. Okuno, Y. Yamato, J. Taniguchi, N. Wada, S. Inagaki, and Y. Fukushima, Film growth of ^{4}He adsorbed in mesopores, Phys. Rev. B **68**, 092501 (2003).
[30] H. Godfrin, M. Meschke, H.-J. Lauter, A. Sultan, H. M. Böhm, E. Krotscheck, and M. Panholzer, Observation of a roton collective mode in a two-dimensional Fermi liquid, Nature **483**, 576 (2012).
[31] J. Taniguchi, T. Okuno, H. Ikegami, and N. Wada, Vapor pressure and heat capacity measurement of 3he adsorbed on 18Å-pores, J. Low Temp. Phys. **126**, 259 (2002).
[32] N. Wada, T. Matsushita, R. Toda, Y. Matsushita, M. Hieda, J. Taniguchi, and H. Ikegami, One-dimensional ^{4}He and ^{3}He quantum fluids realized in nanopores, AIP Conference Proceedings **850**, 289 (2006).
[33] A. Evenson, D. Brewer, A. Symonds, and A. Thomson, Van der waals potential for helium adsorbed on glass and nitrogen coated glass, Physics Letters A **33**, 35 (1970).
[34] F. Pobell, *Matter and Methods at Low Temperatures, section 4.3* (Springer-Verlag, Berlin, 2007).
[35] H. Franco, J. Bossy, and H. Godfrin, Properties of sintered silver powders and their application in heat exchangers at millikelvin temperatures, Cryogenics **24**, 477 (1984).
[36] M. Watanabe, M. Morishita, and Y. Ootuka, Magnetoresistance of RuO_2-based resistance thermometers below 0.3 K, Cryogenics **41**, 143 (2001).
[37] J. S. Xia, L. Yin, E. D. Adams, and N. S. Sullivan, A compact capacitive pressure transducer, J. of Phys.: Conf. Series **150**, 012054 (2009).
[38] N. S. Nichols, T. R. Prisk, G. Warren, P. Sokol, and A. Del Maestro, Dimensional reduction of helium-4 inside argon-plated MCM-41 nanopores, Phys. Rev. B **102**, 144505 (2020).
[39] D. M. Silver, Interaction energy between two ground-state helium atoms using many-body perturbation theory, Phys. Rev. A **21**, 1106 (1980).
[40] T. Matsushita, K. Kurebayashi, R. Shibatsuji, M. Hieda, and N. Wada, Possible dimensional crossover to 1D of ^{3}He fluid in nanochannels observed in susceptibilities, J. Low Temp. Phys. **183**, 10.1007/s10909-015-1369-8 (2016).
[41] J. Xu, O. Avenel, J. S. Xia, M.-F. Xu, T. Lang, P. L. Moyland, W. Ni, E. D. Adams, G. G. Ihas, M. W. Meisel, N. S. Sullivan, and Y. Takano, Nuclear demagnetization cryostat at University of Florida Microkelvin Laboratory, J. Low Temp. Phys. **89**, 719 (1992).
[42] N. Sullivan, J. Xia, E. Adams, G. Boebinger, and H. Schneider-Muntau, The National High Magnetic Field Laboratory Ultra-High B/T Facility, Physica B, Cond. Matt. , 519 (2001).
[43] A. Shekhar, R. K. Kalia, A. Nakano, P. Vashishta, C. K. Alm, and A. Malthe-Sørenssen, Universal stretched exponential relaxation in nanoconfined water, Appl. Phys. Lett. **105**, 161907 (2014).
[44] M. Thill and D. Huse, Equilibrium behaviour of quantum Ising spin glass, Physica A **214**, 321 (1995).
[45] J. C. Phillips, Stretched exponential relaxation in molecular and electronic glasses, Repts on Prog. in Phys. **59**, 1133 (1996).
[46] O. Edholm and C. Blomberg, Stretched exponentials and barrier distributions, Chemical Physics **252**, 221 (2000).
[47] J. Klafter and M. F. Shlesinger, On the relationship among three theories of relaxation in disordered systems, Proc. Nat. Acad. Sci. **83**, 848 (1986).
[48] D. S. Fisher and D. A. Huse, Ordered phase of short-range Ising spin-glasses, Phys. Rev. Lett. **56**, 1601 (1986).
[49] D. S. Fisher and D. A. Huse, Nonequilibrium dynamics of spin glasses, Phys. Rev. B **38**, 373 (1988).